

STUDY OF ONE AND TWO-NEUTRON TRANSFER REACTIONS

ON ^{27}Al USING ^{18}O AND ^{13}C BEAMS

446
1226-5600

by

STEVEN A. SCHILLER

B.S., St. Norbert College, 1971

A MASTER'S THESIS

submitted in partial fulfillment of the

requirements for the degree

MASTER OF SCIENCE

Department of Physics

KANSAS STATE UNIVERSITY
Manhattan, Kansas

1973

Approved by:

John D. Eck
Major Professor

LD
2668
T4
1973
S3
C.2
Doc.

11

To all of the people back home in Port Washington, Wisconsin who often quipped "Send you to school, buy you books, and you still don't know a darn thing".

TABLE OF CONTENTS

	PAGE
LIST OF TABLES	v
LIST OF FIGURES	vi
CHAPTER	
I. INTRODUCTION	1
II. EXPERIMENTAL TECHNIQUE	3
A. Beam	3
B. Target	3
C. Chamber	3
D. Electronics	5
E. Data Acquisition	5
F. Half-life Measurement	9
III. ANALYSIS	10
A. Cross Section Determination	10
B. Beam-Off Spectra Selection	11
C. Relative Yield	17
D. Detector Efficiency and Solid Angle	17
E. Charge Conversion and Normalized Yield	18
F. Target Thickness	18
G. Cross Section Calculation	19
IV. DISCUSSION	25
A. Error Considerations	25
B. Shell Model Description of ^{18}O and ^{13}C	28
C. Centrifugal Barrier Discussion	30
D. Possible Structure	32

TABLE OF CONTENTS (continued)

CHAPTER	PAGE
V. CONCLUSION	33
REFERENCES	35
ACKNOWLEDGEMENTS	37
VITA	38
ABSTRACT	

LIST OF TABLES

TABLE	PAGE
I. Possible Sources of Beam-On Gamma Rays	14
II. Shell Model Ground State Configurations of ^{13}C , ^{18}O , and ^{27}Al	29

LIST OF FIGURES

FIGURE	PAGE
1. Drawing of the Chamber Showing Position of the Ge(Li) Detector	4
2. Gamma Ray Spectra of ^{18}O on ^{27}Al Comparing the Beam-On and Beam-Off Spectra	6
3. Block Diagram of the Timing and Electronic Configuration Used in the Gamma Ray Experiment	8
4. 4096 Channel Gamma Ray Beam-On and Beam-Off Spectra for ^{18}O on ^{27}Al	12
5. Energy Levels and Decay Schemes of ^{28}Al and ^{29}Al	15
6. Cross Section for $^{27}\text{Al}(^{18}\text{O}, ^{17}\text{O})^{29}\text{Al}$ Reaction Using ΔE 's of 2, 3, 4, and 5	22
7. Cross Section for $^{27}\text{Al}(^{18}\text{O}, ^{16}\text{O})^{29}\text{Al}$ Reaction Using ΔE 's of 2, 3, 4, and 5	23
8. Comparison of $^{27}\text{Al}(^{18}\text{O}, ^{17}\text{O})^{28}\text{Al}$ and $^{27}\text{Al}(^{13}\text{C}, ^{12}\text{C})^{28}\text{Al}$ Cross Sections Using a ΔE of 2	26
9. Comparison of $^{27}\text{Al}(^{18}\text{O}, ^{16}\text{O})^{29}\text{Al}$ and $^{27}\text{Al}(^{18}\text{O}, ^{17}\text{O})^{28}\text{Al}$ Cross Sections Using a ΔE of 2	27

I. INTRODUCTION

The nuclear interaction of heavy ions has been studied with increasing vigor in recent years. The information from these various types of reactions shows the presence of effects not seen in light ion reactions.^{1,2,3} Among the numerous types of experiments being performed with heavy ions are transfer reactions.

A transfer reaction is one in which one or more of the particles composing the bombarding nucleus are removed from the projectile and are attached to the target nucleus. The nature of these transfer reactions is strongly dependent on the structure of the projectile and target nuclei.

The properties of the final nucleus which is formed determine the type of experiment that is performed. If a total cross section is required often a gamma ray experiment can be used, or if a differential cross section is needed a particle scattering experiment is preferred. Proper selection of the target and projectile determine the amount of information which may be obtained.

The specific transfer reactions that this work concerns itself with are $^{27}\text{Al}(^{18}\text{O}, ^{16}\text{O})^{29}\text{Al}$, and $^{27}\text{Al}(^{18}\text{O}, ^{17}\text{O})^{28}\text{Al}$ in the lab energy range from 24 to 34 MeV. The reaction $^{27}\text{Al}(^{13}\text{C}, ^{12}\text{C})^{28}\text{Al}$ was also examined in the energy range 16 to 26.5 MeV.

By bombarding ^{27}Al with ^{18}O , one and two neutron transfer reaction cross sections were measured as a function of the ^{18}O bombarding energy. ^{13}C was also used as a projectile on the ^{27}Al and the one neutron transfer reaction cross section was measured as a function of the ^{13}C bombarding energy. Converting the bombarding energies to the center

of mass system allowed the comparison of the one-neutron transfer cross sections for the $^{27}\text{Al}(^{18}\text{O}, ^{17}\text{O})^{28}\text{Al}$ and $^{27}\text{Al}(^{13}\text{C}, ^{12}\text{C})^{28}\text{Al}$ reactions.

The information obtained is indicative of the structure of the ^{18}O and ^{13}C nuclei and also the ease with which the one and two extra neutrons attached themselves to the ^{27}Al target nuclei. The resulting cross section determinations for the $^{27}\text{Al}(^{18}\text{O}, ^{16}\text{O})^{29}\text{Al}$, $^{27}\text{Al}(^{18}\text{O}, ^{17}\text{O})^{29}\text{Al}$, and $^{27}\text{Al}(^{13}\text{C}, ^{12}\text{C})^{28}\text{Al}$ reactions can be compared relative to one another with respect to what might be expected from shell model considerations. The relative ease with which the experiment could be performed and the general statements that could be made concerning the data using a simple analysis provided the incentive to investigate the aforementioned reactions.

II. EXPERIMENTAL TECHNIQUE

A. Beam

A diode ion source was used to obtain the ^{18}O and ^{13}C beams. For the ^{18}O beam, liquid water, (enriched to sixteen percent H_2^{18}O) was placed in a glass tube which was evacuated and the resulting water vapor was introduced into the source. The ^{13}C beam was obtained by introducing ^{13}CN gas into the diode source.

A Model EN Tandem Van de Graaff accelerator was then used to accelerate ^{18}O and ^{13}C beams. A 5+ charge state ^{18}O beam with lab energies from 24 to 34 MeV and 4+ ^{13}C beam with an energy range of 16 to 26.5 MeV in the lab were utilized.

B. Target

The target was a disk one inch in diameter made from one mil aluminum foil which was thick enough to stop the highest energy particle of ^{18}O and ^{13}C . A 26.5 MeV ^{13}C particle is stopped in 0.85 mil of ^{27}Al and a 34 MeV ^{18}O particle in 0.7 mil.⁴

C. Chamber

The chamber used in this gamma ray experiment was of simple construction. Of major concern in its design was the elimination of aluminum to avoid background Al gamma ray production.

The stainless steel chamber shown in Figure 1, was constructed in the shop at Kansas State University. The twenty inch section of stainless steel pipe positioned the chamber in close proximity to the detector. A tantalum collimator was placed just ahead of the chamber

**THIS BOOK
CONTAINS
NUMEROUS PAGES
WITH DIAGRAMS
THAT ARE CROOKED
COMPARED TO THE
REST OF THE
INFORMATION ON
THE PAGE.**

**THIS IS AS
RECEIVED FROM
CUSTOMER.**

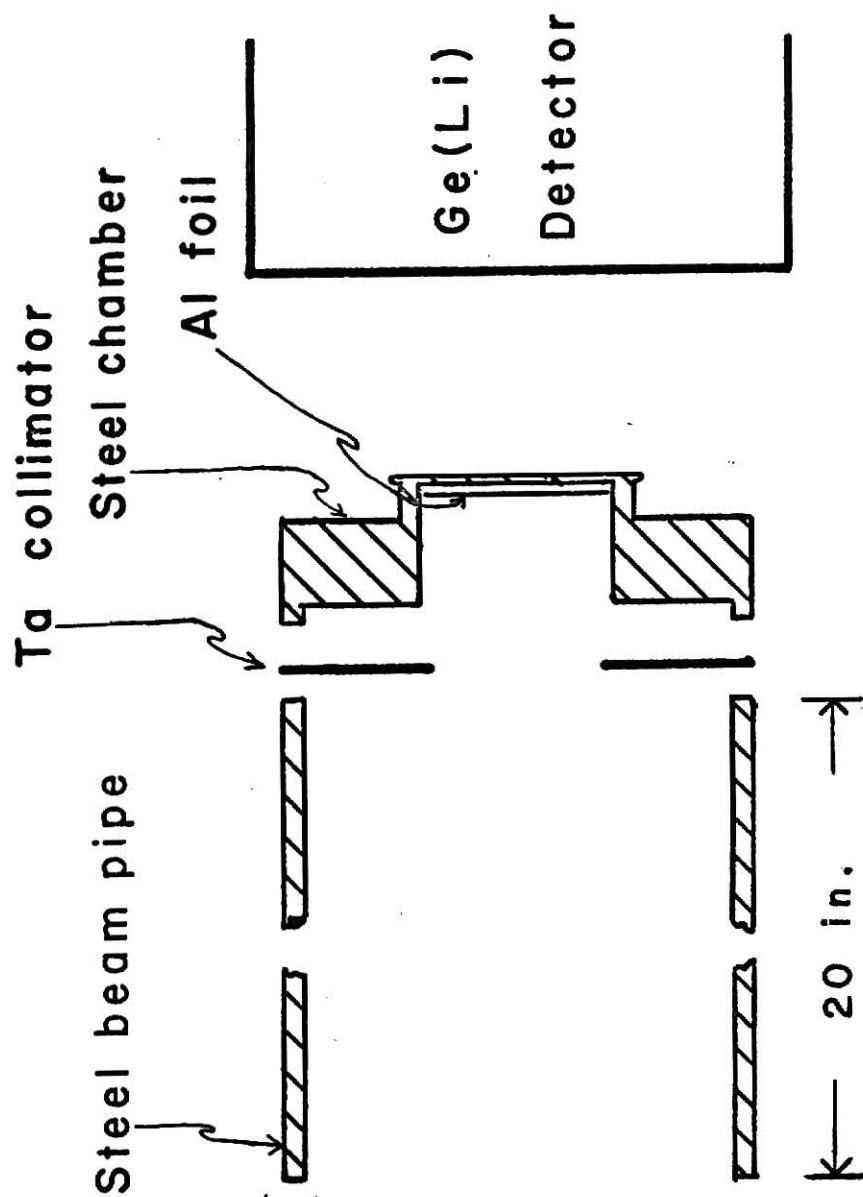


Figure 1. Drawing of the chamber showing relative position of the Ge(Li) detector. Chamber is drawn to actual size.

in contact with the stainless steel beam pipe to allow the beam to only strike the target. The chamber and steel pipe were electrically insulated from the beam line. In order to obtain clean gamma ray spectra, the beam on the target was maximized and the current on the collimator was minimized. The tantalum collimator also did not give off gamma rays which are energetically close to those produced in the transfer reactions. An added advantage of the chamber was its small volume lending itself to rapid pumping.

D. Electronics

The chamber construction allowed the positioning of the Ge(Li) detector directly behind the chamber as is illustrated in Figure 1. Pulses from the detector pre-amp were further amplified using a spectroscopy amplifier (Ortec 451) and then accumulated in a TMC multichannel analyzer. The spectra were spread over 4096 channels. These spectra were then stored on magnetic tape using the Digital Equipment Corporation PDP-15 computer.

E. Data Acquisition

The $^{27}\text{Al}(^{18}\text{O}, ^{17}\text{O})^{28}\text{Al}$, $^{27}\text{Al}(^{18}\text{O}, ^{16}\text{O})^{29}\text{Al}$ and $^{27}\text{Al}(^{13}\text{C}, ^{12}\text{C})^{28}\text{Al}$ reactions were observed by measuring the gamma ray yields following beta decay of ^{28}Al and ^{29}Al . Since the half-lives of the ^{28}Al and ^{29}Al were long, on the order of minutes, it was advantageous to bombard the target for a fixed time, shut the beam off and then accumulate the spectrum. A comparison of gamma ray spectra for ^{18}O bombarding ^{27}Al is shown in Figure 2. The beam-on and beam-off spectra are both shown in the same

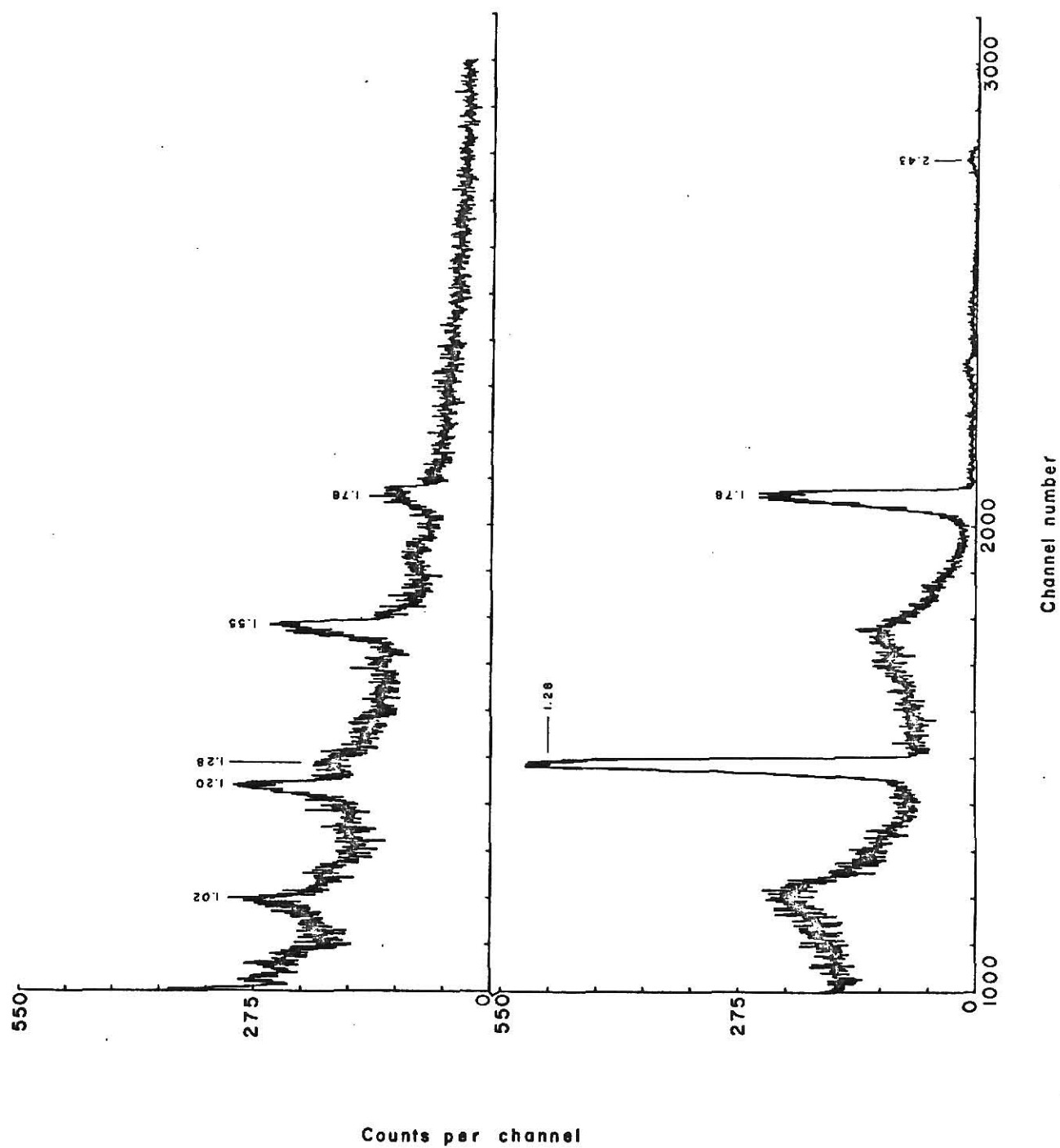


Figure 2. Gamma Ray spectra of $^{18}\text{O} + ^{27}\text{Al}$ comparing the beam-on (upper) and beam-off (lower) spectra over similar energy regions.

energy range. The 1.28 MeV peak which arises from the beta decay of ^{29}Al to the first excited state of ^{29}Si which in turn emits a 1.28 MeV gamma ray,⁵ is hard to distinguish from the background in the beam-on spectrum. In the beam-off spectrum however the peak to background ratio is considerably larger. This makes determining the gamma ray yield a much simpler matter for the beam-off case. This procedure also works for the 1.78 MeV peak, which corresponds to the beta decay of ^{29}Al to the first excited state of ^{28}Si followed by a 1.78 MeV gamma ray.

The target was bombarded, the beam steered away and a spectrum accumulated. The energy of the beam was then changed and the process started again. In order that the accumulation time for each spectrum be the same, a timing and electronic configuration like that shown in Figure 3 was used. This enabled the target to be bombarded for a predetermined amount of time and the multichannel analyzer to count for the same fixed amount of time.

At the beginning of each run the master scaler was started, causing the switching box to switch back to A. The output from the switching box was a continuous five volt dc level in either channel A or B. This in turn would stop the Y-deflection, steer the beam on target, and simultaneously start the scaler counting pulses from the current integrator. During this time the TMC would not be accumulating. After the predetermined time had again elapsed the master scaler would send another pulse which would change the switching box from A to B, which steered the beam away and stopped the scaler from counting and start the TMC accumulating. This was done only once per energy setting. The process

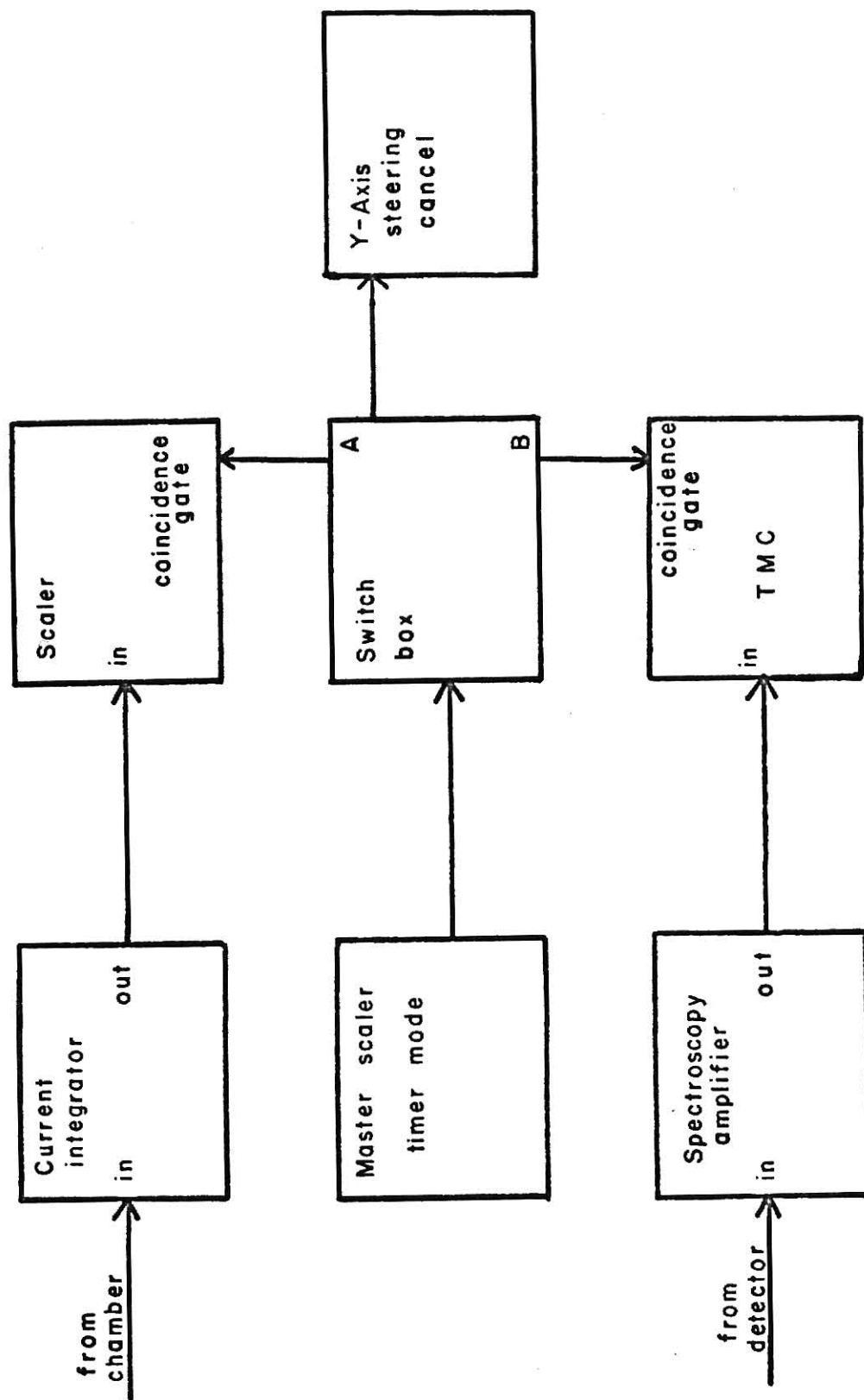


Figure 3. Block diagram of the timing and electronic configuration used the gamma ray experiment.

was stopped after the accumulation of the spectrum.

F. Half-life Measurement

In order to positively insure that the gamma rays observed in the beam-off spectrum were the result of beta decay of ^{28}Al and ^{29}Al , it was necessary to determine that these gamma rays had the correct half-life. To measure the half-life, a window was set, using a single channel analyzer, on each peak. The target was bombarded and then the beam steered away. A scaler was set up to count the number of gamma ray pulses that were contributed to a single peak in a ten-second interval. The value was recorded and the scaler reset. This process was continued until the number of counts contributed in the successive ten-second periods dropped to one-half the original value. When these values were plotted on semi-log graph paper a straight line resulted, from which the half-life was determined.

The half-life determination also decided the amount of time that was selected to bombard the target and to accumulate the spectrum. The concern was to bombard until saturation was reached and to count until the majority of the excited states decayed.

III. ANALYSIS

A. Cross Section Determination

The equation for the number of events expected when a beam of particles strikes a target is written in an equation of the form:⁶

$$Y = s' \sigma Q \quad (1)$$

where Q = number of incident particles
 σ = cross section (cm^2)
 s' = thickness (number of target nuclei/ cm^2)
 Y = yield

To solve for σ , the total cross section one obtains equation (2)

$$\sigma = \frac{Y}{s'Q} \quad (2)$$

To obtain the cross section one must determine each of the factors on the right hand side of equation (2).

However since the spectra were taken with the beam off, the number of ^{28}Al and ^{29}Al that decayed while the beam was on and the analyzer was not counting had to be taken into consideration to obtain the correct yield. The assumption that was made, by choosing a bombarding time of twenty minutes, was that saturation was reached for the 6.6 minute beta decay of ^{29}Al , the longer of the two beta decay half-lives. That is, it was assumed that the number of states being created equalled the number of states decaying. To express this in equation form the following is obtained:

$$\frac{dY_d}{dt} = Y_a(t) \lambda - \frac{Y}{t} = \frac{dY_c}{dt} \quad (3)$$

where Y_d = # destroyed
 Y_c = # created
 Y_a = # actual

At saturation, $Y_a(t)$ is a constant and can be called Y_a without the function of t notation. Equation (1) substituted for Y in equation (3) yields:

$$Y_a = \frac{s' \sigma Q}{\lambda t} \quad (4)$$

λ is the decay constant for the particular nucleus and is defined as $1/\tau$, where τ is the lifetime. Putting this in equation (4) gives the yield corrected for the number of states that decayed while the beam was on.

$$Y_a = s' \sigma Q \frac{\tau}{t} \quad (5)$$

or solving for σ

$$\sigma = \frac{Y_a t}{s' Q \tau} \quad (6)$$

It is essential that the t/τ factor be included to account for the nuclei which decay while the beam is on target and the analyzer is not accumulating.

This factor was of great importance for the 2.3 minute half-life beta decay of ^{28}Al in the $^{27}\text{Al}(^{18}\text{O}, ^{17}\text{O})^{28}\text{Al}$ reaction, since the data for the yield was taken simultaneously with $^{27}\text{Al}(^{18}\text{O}, ^{16}\text{O})^{29}\text{Al}$ reaction data. Because of the 2.3 minute half-life of ^{29}Al and the decision to count for twenty minutes, the effect of the t/τ value was non-negligible for the $^{29}\text{Al}(^{18}\text{O}, ^{17}\text{O})^{28}\text{Al}$ reaction.

B. Beam-Off Spectra Selection

The comparison shown already in Figure 2 and the 4096 channel spectra shown in Figure 4 of beam-on and beam-off spectra for ^{18}O bombarding ^{27}Al give a clear indication of what happens to the background and peaks when the beam-off spectrum is used. In the beam-off spectrum

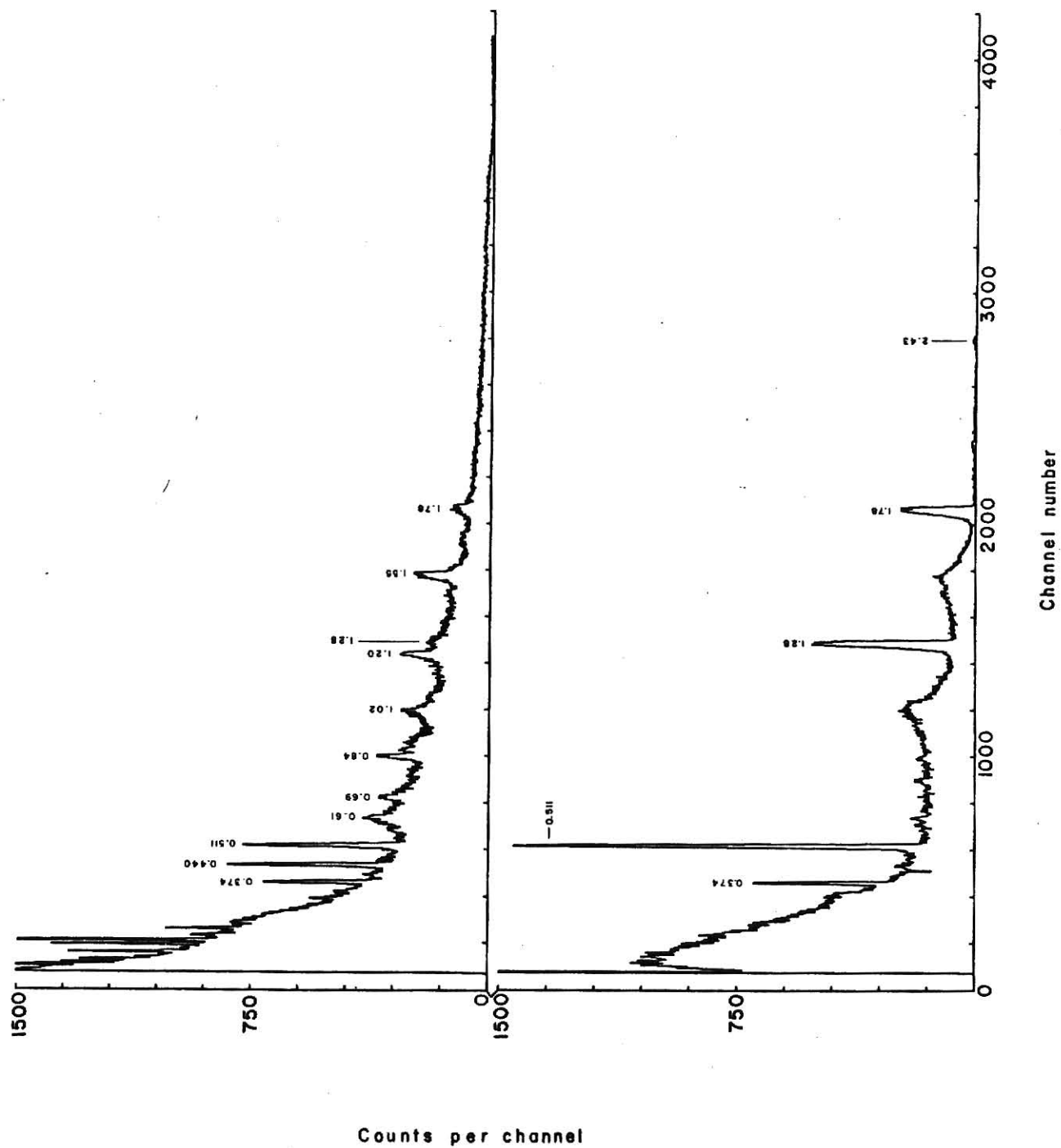


Figure 4. 4096 channel gamma ray beam-on (upper) and beam-off (lower) spectra for ^{18}O on ^{27}Al .

the larger peak to background ratio facilitates analysis.

An attempt was made to identify the peaks in both the beam-on and beam-off spectra. Table I lists the peaks that have been identified in the beam-on spectrum. The gamma ray at 0.84 MeV is of importance to the description of the experiment. The first excited state of ^{27}Al lies 0.842 MeV above the ground state. The first excited state of ^{56}Fe lies at 0.847 MeV above its ground state. To resolve energy differences this small with the Ge(Li) detector used was not possible. To make sure that the primary contributor to the 0.84 MeV peak was from the ^{27}Al and not the ^{56}Fe , that is that the collimation allowed the beam to see only the target, a comparison of a spectrum of ^{18}O on ^{28}Si to a spectrum of ^{18}O on ^{27}Al was made. The 0.84 peak was considerably smaller in the ^{18}O on ^{27}Al case. This ensured that the beam was striking only the target.

In the beam off spectrum the four prominent and two less prominent lines are at 0.374, 0.511, 1.28, 1.78, 2.03, 2.43 MeV. This led one to investigate what possible reactions with ^{18}O bombarding ^{27}Al had these gamma rays and were also sufficiently long lived in order to detect them with the beam off.

The only reactions that had long lived states⁷ were $^{27}\text{Al}(^{18}\text{O}, ^{16}\text{O})^{29}\text{Al}$, $^{27}\text{Al}(^{18}\text{O}, ^{17}\text{O})^{28}\text{Al}$, and $^{27}\text{Al}(^{18}\text{O}, 2n)^{43}\text{Sc}$. The ^{29}Al has a half-life of 6.6 minutes and then beta decays to ^{29}Si which emits 1.28(90%), 2.03(4%), and 2.43(6%) MeV gamma rays. The ^{28}Al has a 2.3 minute half-life and then beta decays to ^{28}Si which emits a 1.78 MeV gamma ray. Both the ^{28}Si and ^{29}Si gamma ray half-lives are of the order of picoseconds, so that the gamma rays appear to have the half-lives of the beta decay of 2.3 and 6.6 minutes respectively. The energy level schemes shown in Figure 5 display the gamma ray transitions involved. The relative strengths of the

<u>γ-Energy (MeV)</u>	<u>Possible Nuclei or Source</u>
0.374	$^{43}_{20}\text{Ca}$
0.440	$^{23}_{11}\text{Na}$
0.511	annihilation radiation
0.61	$^{43}_{20}\text{Ca}$
0.69	?
0.84	$^{27}_{13}\text{Al}$ or $^{56}_{26}\text{Fe}$
1.02	$^{27}_{13}\text{Al}$
1.20	?
1.28	$^{29}_{14}\text{Si}$
1.55	$^{43}_{20}\text{Ca}$
1.78	$^{28}_{14}\text{Si}$

Reference C. M. Lederer, J. M. Hollander and I. Perlman, Table of Isotopes, (John Wiley and Sons, Inc., New York, 1968).

Table I. List of strong gamma rays in beam-on spectrum shown in Figure 4.

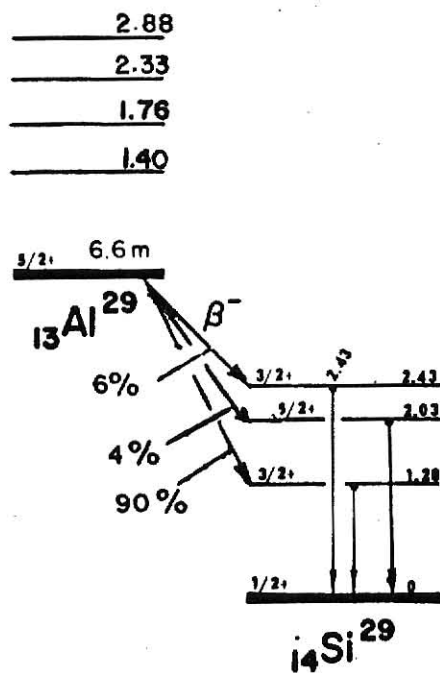
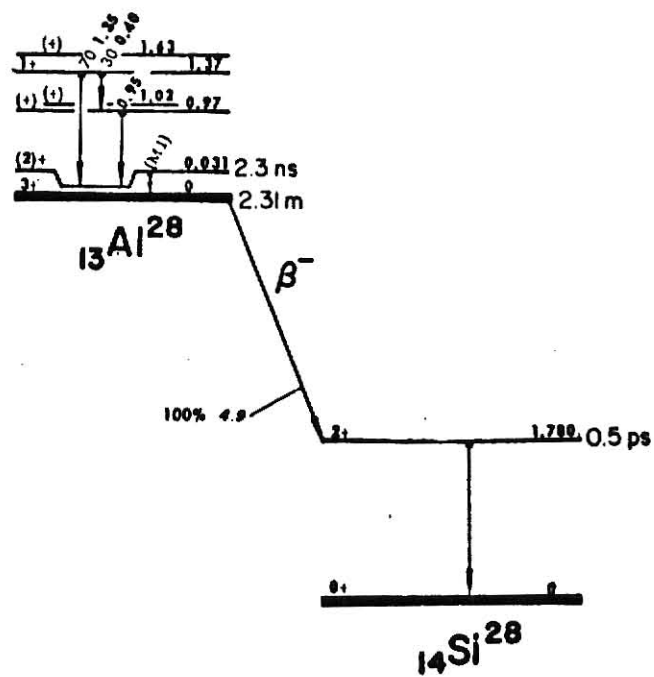


Figure 5. Energy levels and decay schemes of ^{28}Al and ^{29}Al .

^{29}Al beta decays channels to ^{29}Si were corrected from those given in the Table of the Isotopes by Lederer.⁸ More recent work by W. R. Harris et al.⁹ yielded the values shown. The energy level scheme of ^{29}Al has been inserted also.¹⁰ The peak at 2.03 MeV is not labeled on Figure 4 but would be near channel number 2400. It is perhaps easier to see this in Figure 2, which is a 1000 channel portion of the spectra shown in Figure 4.

One other peak in the beam off spectrum was at 0.374 MeV. This is due to ^{43}Sc , which is produced in the $^{27}\text{Al}(^{18}\text{O}, 2n)^{43}\text{Sc}$ reaction, with a half-life of 3.9 hours, to ^{43}Ca which then emits a 0.374 MeV gamma ray.¹¹ The 0.511 MeV peak is the everpresent annihilation radiation.

To be certain that the peak at 1.28 MeV was from the first excited state in ^{29}Si populated by the beta decay of ^{29}Al and the peak at 1.78 MeV from the first excited state in ^{28}Si populated by the beta decay of ^{28}Al , the experimental half-life was determined as explained in Chapter II, section F. It was found that the half-life for the 1.28 MeV gamma ray was 6.6 ± 0.2 minutes which agreed well with the ^{29}Al half-life. The half-life of the 1.78 MeV state was found to be 2.3 ± 0.1 minutes again in close agreement with the ^{28}Al half-life. The combination of the proper energy and half-life for both gamma rays confirmed that these resulted from the beta decay of ^{28}Al and ^{29}Al to ^{28}Si and ^{29}Si , respectively.

The peak at 0.374 due to ^{43}Sc beta decaying to ^{43}Ca with its 3.9 hour half-life was not considered. To check on its half-life would have taken a considerable amount of time with the method used here and was not of interest in the cross section measurements. Secondly, the use of ^{18}O water for the long period of time needed to obtain even a few data points was prohibited because of its high cost.

C. Relative Yield

After each spectrum was accumulated it was stored on magnetic tape. Each spectrum was then reread using the program PHAIE on the PDP-15 computer. The program allowed the operator to set a delimiter on either side of a peak and a background marker was also available. By requesting the area, the program would print out the number of events between the background marker and the peak that was set off by the delimiters. This value of the area was be called the relative yield.

The measured relative yield in the 1.28 MeV peak resulting from the decay of the first excited state in ^{29}Si had to be corrected. As was shown in Figure 5 the beta decay of the ^{28}Al also populated the second and third excited states in ^{29}Si corresponding to the 2.03 and 2.43 gamma rays respectively. In order to take the yield in these peaks into consideration, since 10% of the beta decay populated the 2.03 and 2.43 levels implying that only 90% of all the ^{29}Al states formed were observed, a correction to the area in the 1.28 MeV peak was made. To obtain the actual number of ^{29}Al formed, the yield in the 1.28 MeV peak was multiplied by 1.11.

D. Detector Efficiency and Solid Angle

The Ge(Li) detector used is not one hundred percent efficient for detecting the gamma rays of interest, therefore, a correction factor needed to be determined to compensate for this effect. Also the particular geometry of the detector determines the solid angle subtended. A factor combining the two effects is called $\epsilon\Omega$.

Determination of this factor was accomplished by placing a calibrated gamma ray source in the same position as that of the target. Sources were used which gave off gamma rays that bracketed the energy region of

the 1.28 MeV gamma ray from ^{29}Si and the 1.78 MeV gamma ray from ^{28}Si . The ratio of the actual number of gamma rays observed in a fixed amount of time to the expected number of gamma rays was plotted versus the gamma ray energy. Over the region from 1.28 to 1.78 MeV, the factor $\epsilon d\Omega$ was approximately linear and varied by about five percent from 1.28 to 1.78. Specific values of $\epsilon d\Omega$ for the 1.28 MeV gamma ray and for the 1.78 MeV gamma ray were taken from the calibration curve.

E. Charge Conversion and Normalized Yield

The current integrator put out a pulse after a fixed amount of charge had hit the target. The pulses, called integrator counts, were stored in a scaler. The total number of integrator counts was recorded for each data point.

The number of nanocoulombs per integrator count was known by the scale selected on the device. To convert the charge to the number of ^{18}O or ^{13}C particle that had struck the target was a straightforward procedure. Since the charge state, which is fixed by the analyzing magnet, of the ^{18}O was 5+ and that of ^{13}C was 4+, a ratio of the number of nanocoulombs per integrator count to the number of coulombs of charge per ion striking the target was calculated. By taking these values and dividing by the relative yield at that energy, a value which will be called the normalized yield, Y_N , resulted.

F. Target Thickness

The number of collision or the amount of energy lost, that an ^{18}O or ^{13}C atom experienced, depended upon the effective thickness of the target that it passed through. The higher the energy the greater the thickness

of the target the beam observed.

To obtain the information on stopping power versus energy, Northcliffe and Schilling tables were used. Their list gave stopping powers for ^{16}O and ^{12}C beams on ^{27}Al targets. To obtain the correct stopping powers for ^{18}O and ^{13}C on ^{27}Al from the values for ^{16}O and ^{12}C on Al, the values listed for ^{16}O and ^{12}C on ^{27}Al were multiplied by the ratio of the masses of ^{18}O and ^{16}O and ^{13}C to ^{12}C respectively. The values that are listed in their tables were generated by a computer code.

Since the values for the stopping power that were listed were spread out over the energy region of interest, 24 to 34 MeV for ^{18}O and 16.5 to 26 MeV for ^{13}C a curve was fit to the points. The specific values of the stopping power at the energies used were read from the linear plot of stopping power versus energy obtained.

To convert this to atoms per cm^2 , the value that was obtained in each case was multiplied by Avagadro's number and divided by the density of the ^{27}Al target. This value is labelled s.

G. Cross Section Calculation

To compute accurately the cross section as a function of energy, values for yields would have to be obtained for many points that would be separated in energy by small amounts. Essentially the cross section at an energy E can be written as in equation (7).

$$\sigma(E) = \int_0^E d\sigma(E) \quad (7)$$

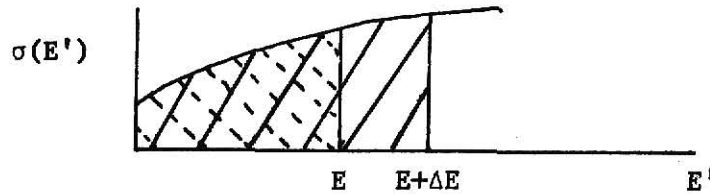
Also for $\sigma(E+\Delta E)$ the expression can be written as in equation (8)

$$\sigma(E+\Delta E) = \int_0^{E+\Delta E} d\sigma(E')$$

If the ΔE is small then the integral signs can be kept and the value for any arbitrary $\sigma(E)$ can be given. However in this experiment the energy of the ^{18}O beam was varied in 0.5 MeV steps from 34 to 26 MeV and in 1.0 MeV steps from 26 to 24 MeV. Similarly for ^{13}C , the energy varied from 26.5 to 20 MeV in 0.5 MeV steps and from 20 to 16 MeV in 1.0 MeV increments. A value for yield was obtained for each energy setting. The ΔE 's are such that the integral equations (7) and (8) can be better used as follows

$$\sigma(E+\frac{\Delta E}{2})\Delta E = \int_0^{E+\Delta E} d\sigma(E') - \int_0^E d\sigma(E') \quad (9)$$

If the cross section is plotted versus energy, $\int_0^E d\sigma(E)$ is represented by the area indicated with dashed lines and $\int_0^{E+\Delta E} d\sigma(E')$ as solid lines, as shown in the following figure:



The region in which only the solid lines are observed closely approximates the left hand side of equation (9). Retrieving equation (6) and incorporating equation (9) the following is obtained:

$$\sigma(E+\frac{\Delta E}{2}) = \frac{\int_0^{E+\Delta E} d\sigma(E') - \int_0^E d\sigma(E')}{\Delta E} = \frac{t}{\tau} \frac{1}{\Delta E} \left(\frac{Y(E+\Delta E)}{Q_{E+\Delta E}} - \frac{Y(E)}{Q_E} \right) \quad (10)$$

To clarify further equation (10) all the factors mentioned earlier are combined and the result is shown in equation (11)

$$\sigma(E + \frac{\Delta E}{2}) = \frac{1}{\epsilon d \Omega} \frac{\rho}{\Delta E} \frac{t}{s N_0 \tau} (Y_N(E + \Delta E) - Y_N(E)) \quad (11)$$

Where $Y_N(E)$ is the normalized yield for energy E

N_0 is avogadro's number

ρ is the density of ^{27}Al

t is the time of bombardment

s is the thickness

τ is the life-time

$\epsilon d \Omega$ is the detector efficiency

Using equation (11), the measured cross sections were obtained for the $^{27}\text{Al}(^{18}\text{O}, ^{16}\text{O})^{29}\text{Al}$, $^{27}\text{Al}(^{18}\text{O}, ^{17}\text{O})^{28}\text{Al}$, and $^{27}\text{Al}(^{13}\text{C}, ^{12}\text{C})^{28}\text{Al}$ reaction data. In order to smooth fluctuations in the data ΔE 's of 2 through 5 MeV were chosen. If the assumptions made were correct the values calculated using the various ΔE 's would tend to average together. Values for the one-neutron transfer reaction using ^{18}O on ^{27}Al are shown in Figure 6. As is easily seen the values seem to be grouped very well. A similar plot is shown in Figure 7 of the two-neutron transfer reaction again using ^{18}O and ^{27}Al .

As ΔE is made larger the cross sections are smoothed further, eliminating any possible information in regards to structure indicated by variations in the measured yield. A disadvantage of using a ΔE of five is that the region over which the cross section results are valid is decreased. Since the cross section was plotted at $E + \frac{\Delta E}{2}$, by choosing a ΔE of 2 the range of the values of the cross section is spread closer to the extent of the original data points,

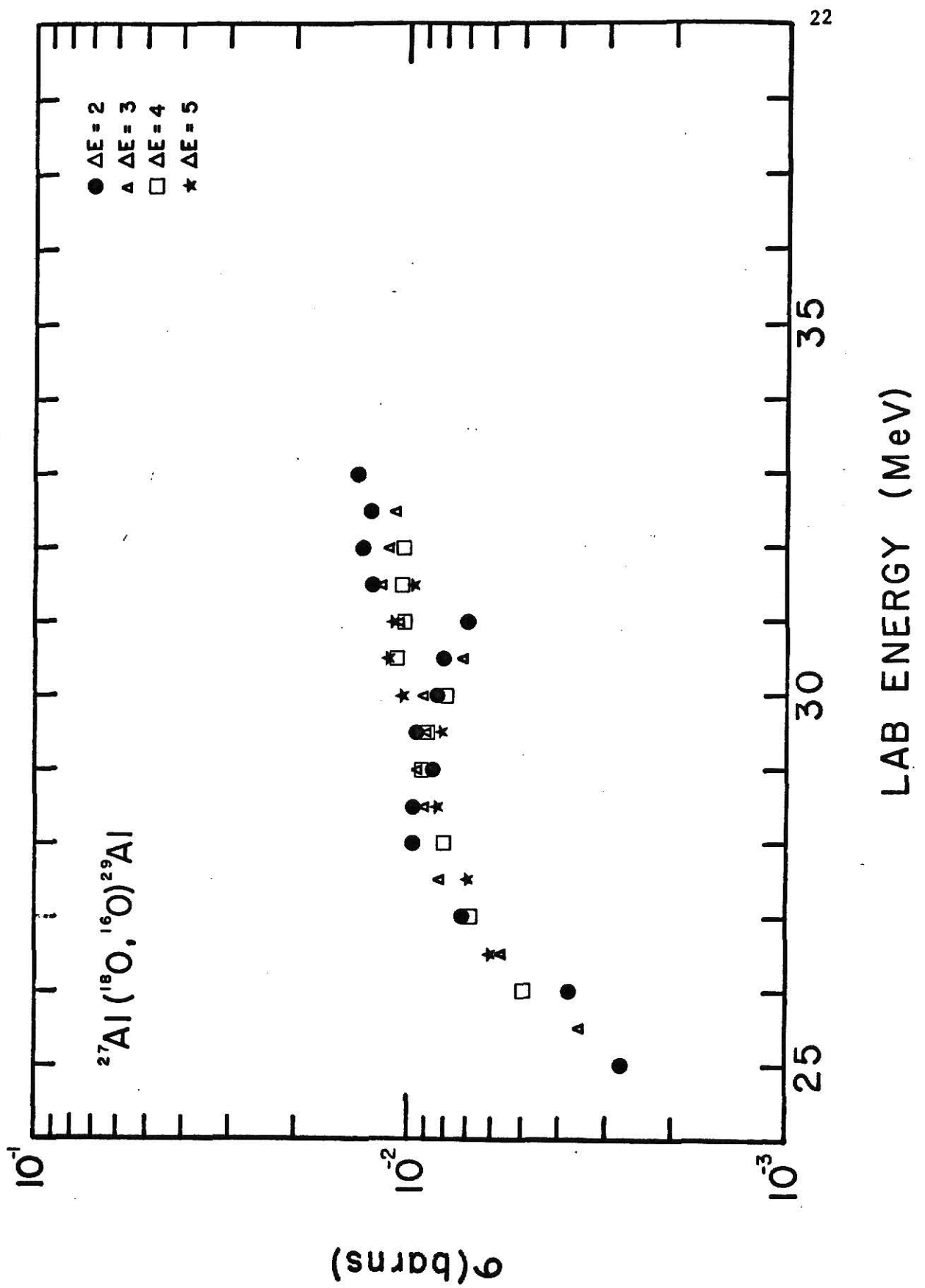


Figure 6. Cross Section for $^{27}\text{Al}(^{18}\text{O}, ^{17}\text{O})^{28}\text{Al}$ reaction using ΔE 's of 2, 3, 4, and 5.

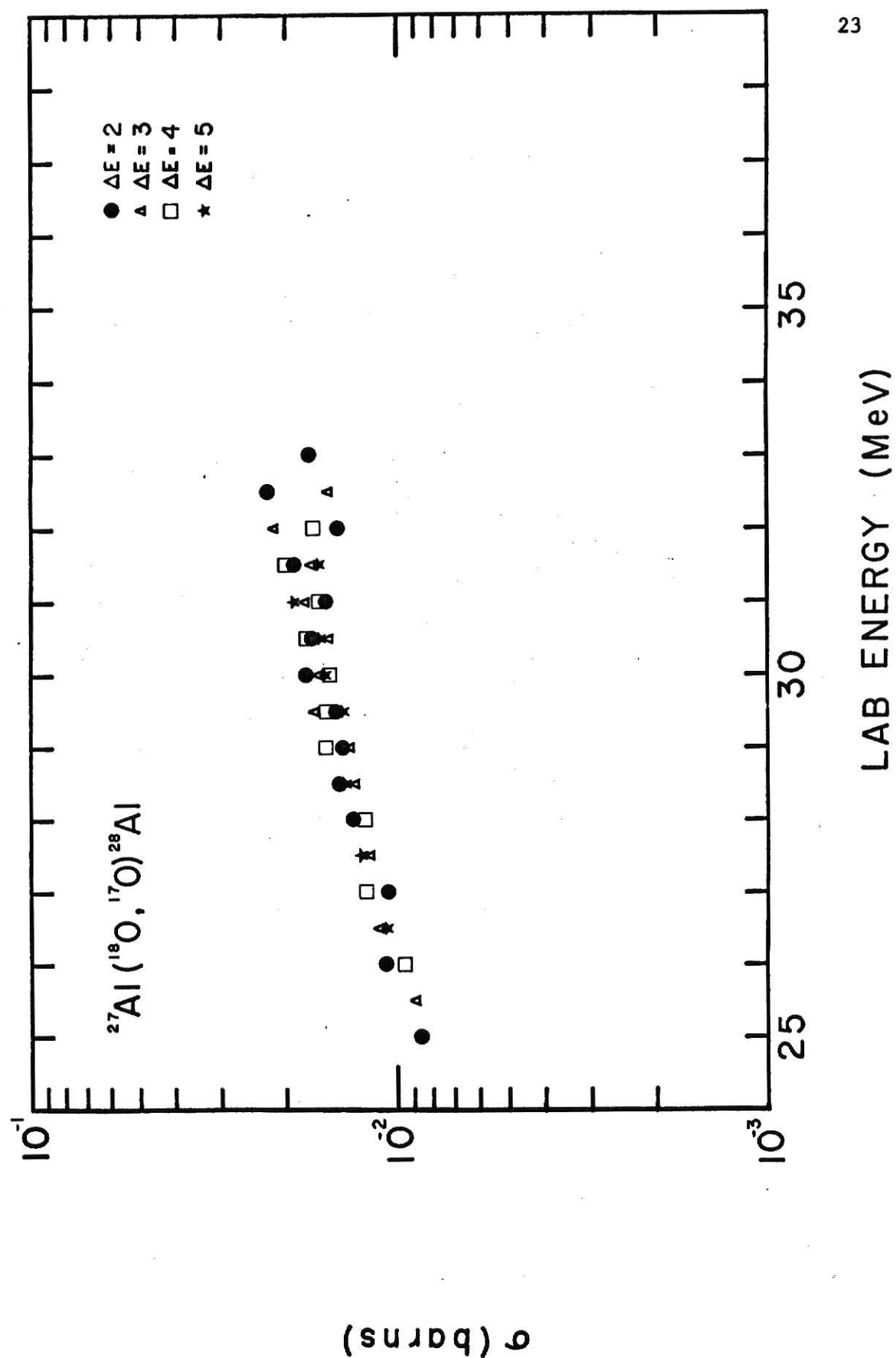


Figure 7. Cross section for $^{27}\text{Al}(^{18}\text{O}, ^{16}\text{O})^{29}\text{Al}$ reaction using ΔE 's of 2, 3, 4, and 5.

than for a ΔE of 5. However any slight changes in the yield due to beam fluctuation or variations in the data will be more strongly observed.

An alternate method for obtaining the values to substitute into equation (11) would be to fit the values for the normalized yield with a least squares program or equivalent. This would have allowed the selection of ΔE 's that are arbitrarily small. However, the program would smooth the data points initially and the values obtained would have been quite similar to those obtained using the data points directly. The fitting would have taken a considerable amount of work more than was required to perform the calculation with the specific values of the normalized yield. It was felt that an equal amount of information could be obtained using the ΔE method and the data points directly.

IV. DISCUSSION

A. Error Considerations

The error bars shown in both Figures 8 and 9 were arrived at in the following manner. The principle source of error was the beam fluctuation. Over the period of twenty minutes, during which the target was being bombarded, the beam fluctuated by about five percent. The effect of the fluctuations was to vary the level of saturation, accounting for the limiting error.

For the stopping power or thickness Northcliffe and Schilling claim an accuracy of one percent¹² for heavy ions. The factor $\epsilon d\Omega$ was determined within three percent and is limited only by the accuracy of the particular source used. Since for saturation, the number of decays observed were really about six percent short, especially for the 1.28 MeV from the first excited state ^{29}Si since the half-life of the ^{29}Al which formed it was 6.6 minutes.

Combining all the errors, a total error of about nine percent is found. For ease in plotting both Figures 8 and 9 indicate the measured cross section plus or minus ten percent.

There should also be a horizontal error bar because of the average technique employed in the calculation. For the $^{29}\text{Al}(^{13}\text{C}, ^{12}\text{C})^{28}\text{Al}$ reaction shown in Figure 8, the horizontal uncertainty would be ± 0.675 MeV in the center of mass system. A ± 0.6 MeV uncertainty is present for both the $^{27}\text{Al}(^{18}\text{O}, ^{17}\text{O})^{28}\text{Al}$ and $^{27}\text{Al}(^{18}\text{O}, ^{16}\text{O})^{27}\text{Al}$ data on both Figures 8 and 9. The reason it is not plotted is that it would have considerably cluttered the plots making the data hard to observe clearly.

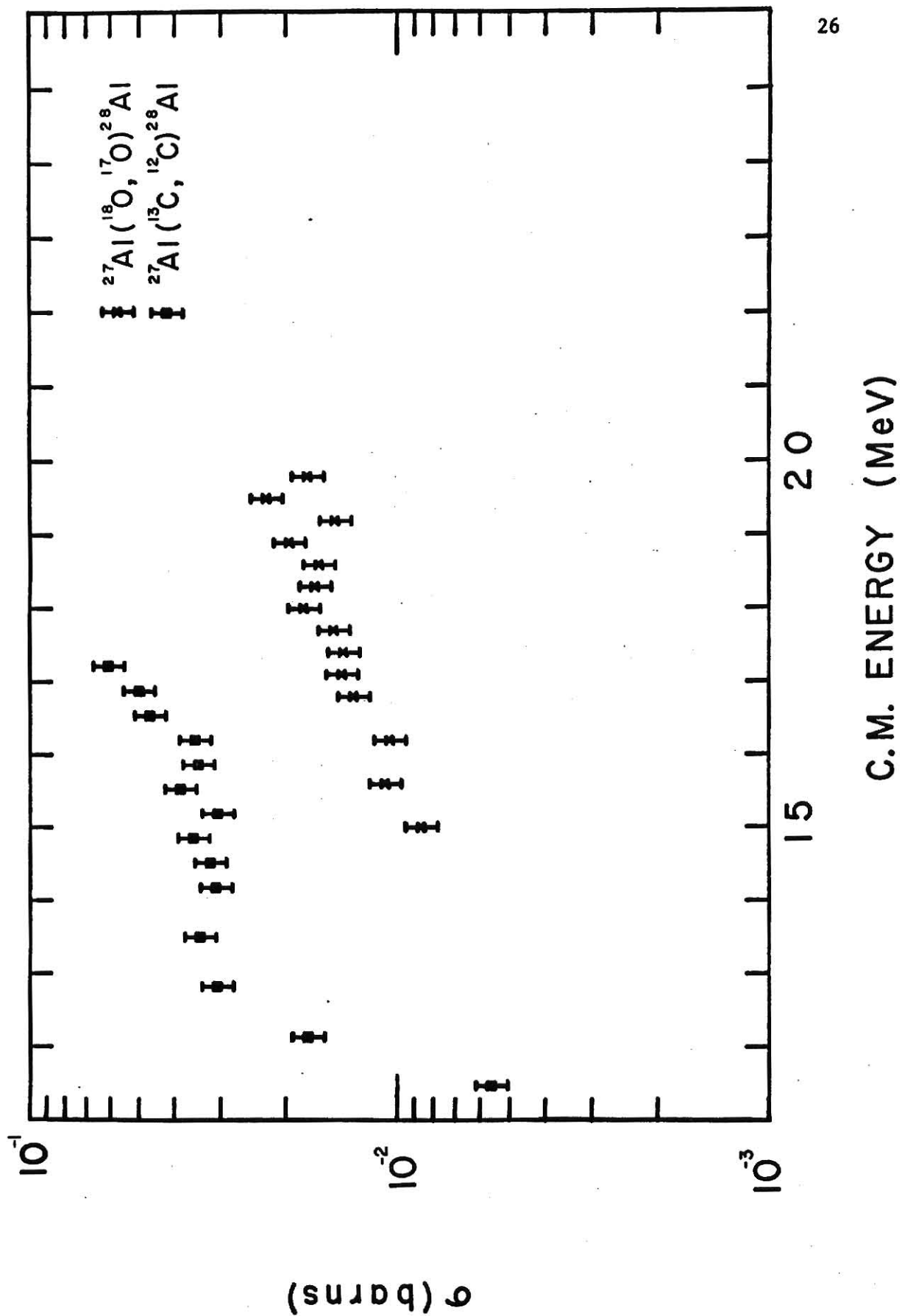


Figure 8. Comparison of $^{27}\text{Al}(^{18}\text{O}, ^{17}\text{O})^{28}\text{Al}$ and $^{27}\text{Al}(^{13}\text{C}, ^{12}\text{C})^{28}\text{Al}$ cross sections using a ΔE of 2.

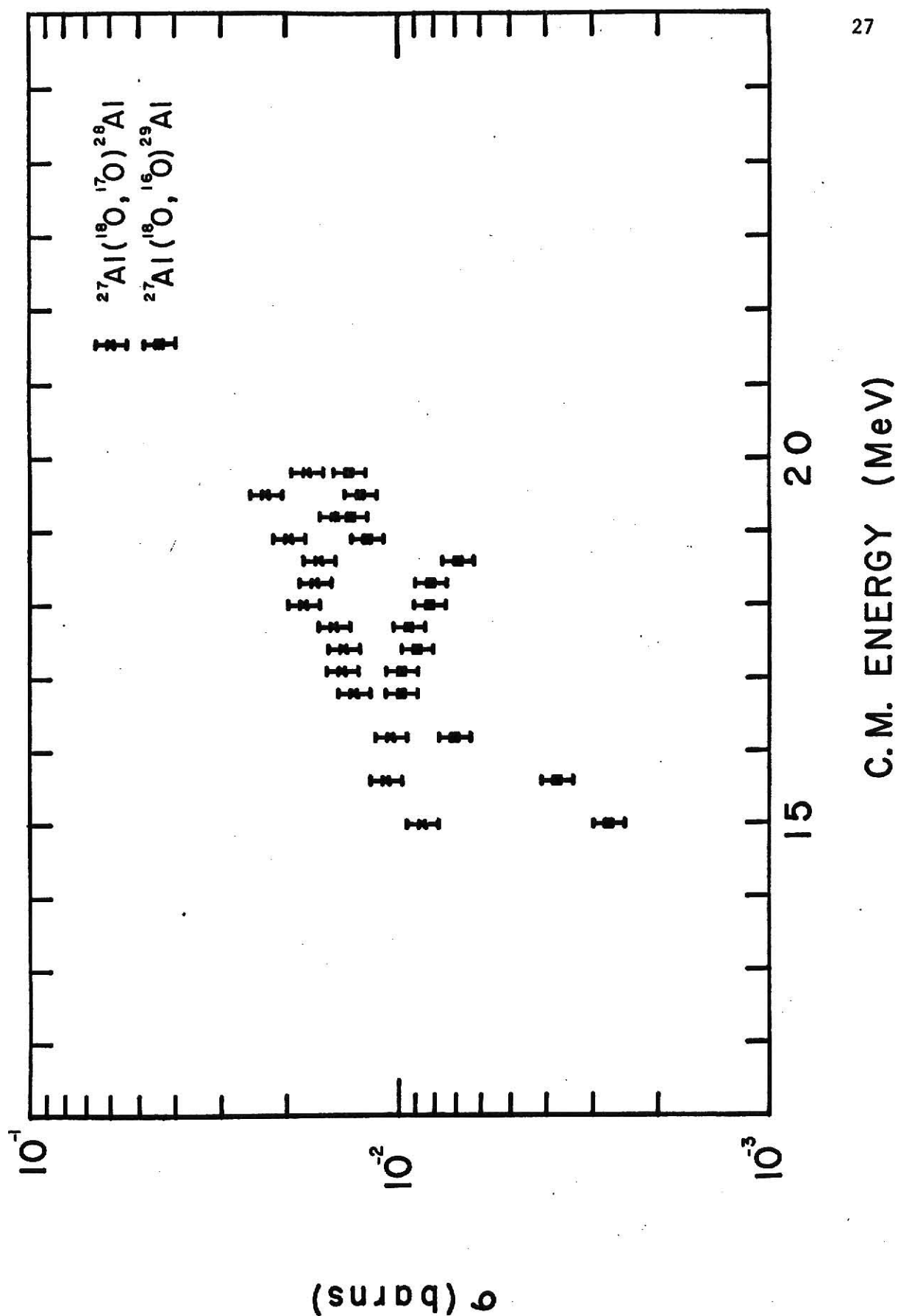


Figure 9. Comparison of $^{27}\text{Al}(^{18}\text{O}, ^{16}\text{O})^{29}\text{Al}$ and $^{27}\text{Al}(^{18}\text{O}, ^{17}\text{O})^{28}\text{Al}$ cross sections using a ΔE of 2.

B. Shell Model Description of ^{18}O and ^{13}C

Using the shell model as a basis the ground state configurations of ^{27}Al , ^{18}O , ^{13}C are shown in Table II. The higher angular momenta levels of a particular state are split in such a way that they lie lower in energy than the lower angular momentum level. The $1p_{3/2}$ and $1p_{1/2}$ levels are a good example.

From the diagram shown in Table II, it can be seen that ^{18}O is the closed shell core of ^{16}O with two extra neutrons in the $1d_{5/2}$ level. ^{13}C , on the other hand, is a ^{12}C core with the extra neutron in the $1p_{1/2}$ level. ^{27}Al has its open neutron levels in the s-d shell. Considering the transfer reactions from an angular momentum standpoint, if just one neutron transfers from the $1d_{5/2}$ level in ^{18}O to the lowest open level in ^{27}Al which is the $2s_{1/2}$ level, a maximum of two units of orbital angular momentum are exchanged. The extra neutrons in the ^{13}C $1p_{1/2}$ level can exchange a maximum of one unit of orbital angular momentum in going into the $2s_{1/2}$ level of ^{27}Al . According to the semi-classical theory, the reaction in which maximum transferred orbital angular momentum is exchanged would lead to a larger transfer reaction cross section.¹³ A comparison of the measured cross section for the $^{27}\text{Al}(^{18}\text{O}, ^{17}\text{O})^{28}\text{Al}$ and $^{29}\text{Al}(^{13}\text{C}, ^{12}\text{C})^{28}\text{Al}$ reaction is shown in Figure 8. It can be noted that just the opposite result is obtained with these data. A factor of five separates the ^{13}C from the ^{18}O one-neutron transfer reaction cross sections.

A second result that is shown in Figure 9 compares the $^{27}\text{Al}(^{18}\text{O}, ^{16}\text{O})^{29}\text{Al}$ and $^{27}\text{Al}(^{18}\text{O}, ^{17}\text{O})^{28}\text{Al}$ transfer reaction cross sections. Using the angular momentum as a consideration again, the two neutrons, assuming that

<u>Element</u>	<u>Protons</u>		<u>Neutrons</u>	
^{13}C	$(1s1/2)^2 (1p3/2)^4$		$(1s1/2)^2 (1p3/2)^4 (1p1/2)$	
^{18}O	$(1s1/2)^2 (1p3/2)^4 (1p1/2)^2$		$(1s1/2)^2 (1p3/2)^4 (1p1/2)^2 (1d5/2)^2$	
^{27}Al	$(1s1/2)^2 (1p3/2)^4 (1p1/2)^2 (1d5/2)^5$		$(1s1/2)^2 (1p3/2)^4 (1p1/2)^2 (1d5/2)^6$	
<hr/>				
$2s\ 1/2$	protons	neutrons	protons	neutrons
	—	—	—	—
	— 0 —	— x x —	—	—
$1d\ 5/2$	— 0 0 —	— x x —	—	—
	— 0 0 —	— x x —	—	—
$1p\ 1/2$	— 0 0 —	— x x —	—	— x —
	— 0 0 —	— x x —	— 0 0 —	— x x —
$1p\ 3/2$	— 0 0 —	— x x —	— 0 0 —	— x x —
	— 0 0 —	— x x —	— 0 0 —	— x x —
$1s\ 1/2$	— 0 0 —	— x x —	— 0 0 —	— x x —
	^{27}Al 13 14	^{18}O 8 10	^{13}C 6 7	

Table II. Shell model ground state configurations of ^{13}C , ^{18}O , and ^{27}Al .

they transferred as a pair, would have a net angular momentum of zero. To transfer the two neutrons to the $2s_{1/2}$ level in ^{27}Al would imply an angular momentum change of zero which is not strongly favored. It is possible they would go to a higher level in the ^{27}Al , however, with the data obtained here it was not possible to distinguish the particular levels populated. If the assumption is made that the neutrons do go to the lowest available state in ^{27}Al it would be expected that the cross section for the one-neutron transfer with ^{18}O would be considerably larger than the two-neutron transfer. Figure 9 indicates that this is not the case for the data obtained, and although the one-neutron transfer cross section is larger than the two-neutron transfer cross section it is not as great as might be expected.

It seems that Figures 8 and 9 yield contradictions to the semi-classical theory. Perhaps a possible explanation for both sets of data would be that the two neutrons in the $1d_{5/2}$ shell of ^{18}O are only partially correlated which implies the wave functions for ^{18}O has a large overlap with both the wave functions of an ^{16}O core and two paired neutrons and an ^{17}O core and one unpaired neutron. In a loose sense this would say that the one and two-neutron transfers measured here would be of about the same order of magnitude. One work,¹⁴ using the stripping reaction $^{18}\text{O}(p,t)^{16}\text{O}$ claimed the interaction of these nuclei was a direct reaction process, tending to confirm the fact that the two neutrons are partially correlated.

C. Centrifugal Barrier Discussion

Even if we do not assume that the ^{18}O is a good shell model nucleus, arguments that are equally plausible to those given for the ^{18}O and ^{13}C

being good shell model nuclei can be made.

Since the one and two-neutron transfer reaction cross sections for the ^{18}O and ^{27}Al are of the same order of magnitude, it would seem to indicate that either the one-neutron transfer cross section is somehow inhibited or the two-neutron transfer somehow enhanced. This assumption is made assuming that the angular momentum considerations work in favor of the one-neutron transfer with ^{18}O on ^{27}Al . If the two neutrons in the s-d shell of ^{18}O were strongly correlated implying a strong pairing interaction, a smaller cross section would be expected. According to recent works by Goldanskii,^{15,16} the effective centrifugal barrier for transfer of a pair of nucleons coupled to $L = 0$ is zero as compared to a finite barrier for a single nucleon transfer with L greater than zero. The transfer probability of a neutron pair with the apparent "switching-off" of the centrifugal barrier may turn out to be very close to the probability of the transfer of one neutron through the centrifugal barrier due to the orbital angular momentum of the one neutron. This would give a very reasonable explanation for the data displayed in Figure 9. The lower angular momentum neutron from the $1p_{1/2}$ level of ^{13}C then would also have a larger cross section than the one neutron transfer from the $1d_{5/2}$ level of ^{18}O because of the centrifugal barrier considerations. The pairing interaction of the two neutrons in ^{18}O would also serve to inhibit the one neutron transfer. The data displayed in Figure 8 is again well explained by the centrifugal barrier considerations.

If the two neutrons in the ^{18}O nucleus are strongly correlated it would imply that it is a poor shell model nucleus. The centrifugal barrier uses this assumption and seems to more easily explain the data.

D. Possible Structure

An effect that is noted in the two-neutron transfer cross section for ^{18}O on ^{27}Al that is not seen in the one-neutron cross section for ^{18}O on ^{27}Al is the large dip in the cross section at $E_{\text{cm}} = 18.5$ MeV as shown in Figure 9. Since the data for the $^{27}\text{Al}(^{18}\text{O}, ^{16}\text{O})^{29}\text{Al}$ and $^{27}\text{Al}(^{18}\text{O}, ^{17}\text{O})^{28}\text{Al}$ reactions were taken simultaneously it may indicate some structure effects. Because the relative population of the various excited states in ^{29}Al or ^{28}Al were not observed in this beam off gamma ray analysis further experiments need to be performed to indicate positively the exact cause of the dip in the data. The dip in the cross section is probably not a result of beam fluctuations since if this were so the yield from the shorter half-life of ^{29}Al would have been more strongly affected than the ^{28}Al .

The cross section data for the $^{27}\text{Al}(^{18}\text{O}, ^{16}\text{O})^{29}\text{Al}$ reaction is of the same order of magnitude as the reaction $^{26}\text{Mg}(^{18}\text{O}, ^{16}\text{O})^{28}\text{Mg}$ performed by Y. Eyal et al.¹² This is important since the ^{26}Mg has the same neutron shell structure as the ^{27}Al and one would expect similar cross sections as a function of energy. Their data does not go to as high an energy to display any possible structure effects as was noted here.

V. CONCLUSION

Because of the relative ease of performing the experiment, and the amount of data that may be obtained in a short amount of time, and the statements that may be made concerning this data, the research done here was quite enjoyable. One of the important considerations to be made in improving the accuracy of the results is to reduce the effect of beam fluctuation. This can be effectively reduced by using a leaky integrator circuit. The integrator circuit is essentially an R-C circuit that has an adjustable time constant which can be varied to match the lifetime of the excited state being observed. The variance of saturation level with beam current would then be eliminated. This would also made the observation of the $^{27}\text{Al}(^{18}\text{O},2n)^{43}\text{Sc}$ reaction and other long lived reactions with hour or day half-lives an easier task.

The technique used in this experiment is not applicable to all nuclei. The formation of nuclei by bombarding one heavy ion on another than have beta decay half-lives on the order of minutes, populating excited states in the subsequent nuclei are limited. The ^{27}Al allows the use of this technique, however the myriad of open levels in the s-d shell does not limit or restrict the possible transitions of the extra neutrons in ^{18}O or ^{13}C . Thus, although the ^{27}Al is experimentally easy to use, a nucleus with a neutron level that would need only one or two neutrons to make the shell complete would be more useful for making more specific statements concerning transfer reactions. ^{14}N and ^{36}Cl are possible targets to investigate the one-neutron transfers of ^{13}C and ^{18}O since there is only one remaining neutron hole in the $1p_{1/2}$ level of ^{14}N and only one in the $1d_{3/2}$ level of ^{36}Cl . If one neutron transferred forming

^{15}N and ^{37}Cl it would not be possible to use a beam-off technique to observe the result, since the half-lives of the states formed would be too short to measure with this experimental set-up.

It is a similar problem for two-neutron hole states in prospective target nuclei. Two examples are ^{12}C and ^{34}S that would enable one to see the strength of one versus two-neutron transfers using the ^{18}O projectile. The problem is that the resulting nuclei ^{14}C and ^{36}S are not well understood in terms of excited states, spins, and parity. Thus to further pursue the data, particle scattering experiments that yield more information with regard to the excited levels would need to be performed.

REFERENCES

1. Proc. Int. Conference on Nuclear Reactions by Heavy Ions, Heidelberg, 1969 (North Holland Publishing Co., 1970).
2. Proc. Sym. Heavy-Ion Scattering, Argonne, 1971 (Argonne Nat. Laboratory, Argonne, Illinois, 1971).
3. Proc. Sym. Heavy-Ion Scattering, Oak Ridge, Tennessee, 1972 (Oak Ridge Nat. Laboratory, Oak Ridge, Tennessee, 1972).
4. L. C. Northcliffe and R. F. Schilling, Nuclear Data Tables, A7 (1970), 265,269.
5. C. M. Lederer, J. M. Hollander, and I. Perlman, Table of Isotopes, (John Wiley and Sons, Inc., New York, 1968), 6 ed., 167.
6. E. B. Paul, Nuclear and Particle Physics, (North Holland Publishing Co., 1969), 96.
7. See Ref. 5, 166, 167, 177.
8. See Ref. 5, 167.
9. W. R. Harris, K. Nagataui, and D. E. Alburger, Phys. Rev., 187, 1445, (1969).
10. A. A. Jaffe, F. de S. Barros, P. D. Forsyth, J. Muto, I. J. Taylor and S. Ramavataram, Proc. Phys. Soc. 76, 914, (1960).
11. See Ref. 5, 177.
12. See Ref. 4, 233.
13. R. A. Broglia and A. Winther, Phys. Letters 4C, 153, (1972).
14. J. C. Legg, Ph.D. Thesis, Princeton University, 1961, (unpublished).
15. V. I. Goldanskii, Yad. Fiz. 1, 596 (1965), Trans. Sov. J. Nucl. Phys. 1, 426 (1965).

16. V. I. Goldanskii, Phys. Letters, 14, 233 (1965).
17. Y. Eyal, I. Dostrovsky, and Z. Fraenkel, Nucl. Phys. A180, 545 (1972).

ACKNOWLEDGEMENTS

The author wishes to acknowledge the many people who have made this work possible. Particularly:

The United States Atomic Energy Commission for sponsoring this research;

Dr. John S. Eck for his ideas, assistance, advice, and encouragement;

Dr. O. L. Weaver and Dr. Louis D. Ellsworth for their helpful discussions;

Mr. Robert Krause and Mr. G. Hartnell for their help in the maintenance and running of the accelerator and computer; and finally

my wife, for her aid, patience, and support.

VITA

Steven A. Schiller, the only child of William T. and Alvina M. Schiller, was born on September 22, 1949 in Port Washington, Wisconsin. He attended Port Washington High School, graduating cum laude in 1967. Subsequently he attended St. Norbert College, De Pere, Wisconsin where he was a member of Delta Epsilon Sigma National Scholastic Honor Society. He obtained a double Bachelor of Science degree in Physics and Mathematics in 1971. His graduate studies at Kansas State University began in the following fall. He acted as a Graduate Teaching Assistant during his first year and a Graduate Research Assistant his second year under the guidance of Dr. John S. Eck. He obtained a Master of Science in Physics at Kansas State University in 1973.

STUDY OF ONE AND TWO-NEUTRON TRANSFER REACTIONS
ON ^{27}Al USING ^{18}O AND ^{13}C BEAMS

by

STEVEN A. SCHILLER

B.S., St. Norbert College, 1971

An abstract of A MASTER'S THESIS

submitted in partial fulfillment of the

requirements for the degree

MASTER OF SCIENCE

Department of Physics

KANSAS STATE UNIVERSITY
Manhattan, Kansas

1973

ABSTRACT

Total cross-sections for the transfer reactions $^{27}\text{Al}(^{18}\text{O}, ^{17}\text{O})^{28}\text{Al}$, $^{27}\text{Al}(^{18}\text{O}, ^{16}\text{O})^{29}\text{Al}$, and $^{27}\text{Al}(^{13}\text{C}, ^{12}\text{C})^{28}\text{Al}$ were measured in the center of mass energy range from 11 - 17.5 MeV for ^{13}C and 14.5 - 20.5 MeV for the ^{18}O , by observing the residual radioactive nuclei $^{28}\text{Al}(\tau_{1/2}=2.31 \text{ minutes})$ and $^{29}\text{Al}(\tau_{1/2}=6.6 \text{ minutes})$. Thick targets of ^{27}Al were bombarded under conditions of constant beam current for a period of 20 minutes for each energy setting. The residual activities were determined by switching the beam off and measuring the yield of 1.28 MeV gamma rays from the first excited state in ^{29}Si and 1.78 MeV gamma ray from the first excited state in ^{28}Si . The ^{28}Si and ^{29}Si are produced by the beta decay of ^{28}Al and ^{29}Al respectively. A comparison of the one-neutron transfer reactions $^{27}\text{Al}(^{13}\text{C}, ^{12}\text{C})^{28}\text{Al}$ and $^{27}\text{Al}(^{18}\text{O}, ^{17}\text{O})^{28}\text{Al}$ and of the one-neutron versus two-neutron transfer reactions $^{27}\text{Al}(^{18}\text{O}, ^{17}\text{O})^{28}\text{Al}$ and $^{27}\text{Al}(^{18}\text{O}, ^{16}\text{O})^{29}\text{Al}$ is made using the shell model as a basis. Taking into account the centrifugal barrier effects described by Goldanskii, a reasonable explanation of the data is presented.